EPSC Abstracts
Vol. 13, EPSC-DPS2019-744-1, 2019
EPSC-DPS Joint Meeting 2019

EPSC
EPSC-DPS Joint Meeting 2019
15–20 September 2019 | Geneva, Switzerland

Similarities and differences of global dust storms in MY 25, 28 and 34 (May-June 2018)

Paulina Wolkenberg (1,2), Marco Giuranna (1), Michael D. Smith (3) and Davide Grassi (1)
(1) Istituto di Astrofisica e Planetologia Spaziali – Istituto Nazionale di Astrofisica (IAPS – INAF), Rome, Italy (paulina.wolkenberg@inaf.it), (2) Centrum Badan Kosmicznych, Polska Akademia Nauk, Warsaw, Poland, (3) NASA, Goddard Space Flight Center, USA

Abstract

We present the observations of dust opacities at 1075 cm^{-1} performed by the Planetary Fourier Spectrometer (PFS) onboard Mars Express (MEx) spacecraft during the global dust storm of MY28 and MY34). The seasonal variations of zonally averaged dust opacities collected from two instruments, the Thermal Emission Spectrometer (TES) and PFS are demonstrated. We investigate the behavior of dust activity before the onset, and during the expansion and decay of GDS in MY 34.

1. Introduction

Global dust storms (GDSs) are peculiar phenomena on Mars. It is still impossible to predict when these events will occur on the planet. In this study we investigate the last three GDSs occurred on Mars.

2. Results

The dataset collected from measurements of TES and PFS contains observations from Ls = 100° in MY 24 to Ls = 300° in MY 34. During this decade we observe three global dust storms in MY 25, MY 28 and MY 34 with dust opacities exceeding 1 (Fig.1). The MY 25 storm is apparently triggered from local dust storms developed at northwestern rim of Hellas at Ls = 177° [1] and expands rapidly to the east at Ls = 185° [1,2]. By Ls = 193° dust encircles the entire planet with lifting centers dominated in Syria/Solis/Daedalia [1,2]. The decay phase starts at Ls = 200.4° and has a duration of 97 sols [3]. The atmospheric clearing lasts until Ls = 304° when nominal seasonal low-levels of dust opacity is reached [3]. The next planet-encircling event occurs in MY 28 (Fig.1). In contrast to that of MY 25, this event starts close to the perihelion season, near Ls = 265°. However, we observe significant dust activities over southern hemisphere before the onset [4]. Dust opacity exceeds 1 over a latitudinal belt between 40°S to 40°N until Ls = 305°.

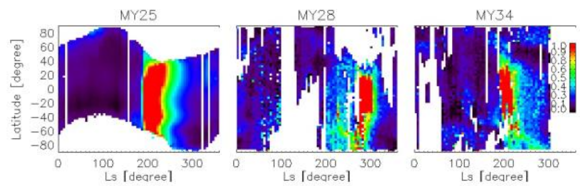

Figure 1: Zonally averaged dust opacities normalized at 6.1 mbar as a function of season and latitude for MY25 (TES-MGS), MY28 and MY34 (PFS-MEx).

Then the decay phase begins, with opacity larger than 0.5 until Ls = 310° [5]. Next global dust storm starts in MY 34 at Ls ~ 190°. The core of this GDS extends from 50°N to the South Pole. Similarities are found in the onset of MY25 and 34 storms while MY 28 storm starts at a different Ls. The common feature of storms in MY 25 and 34 is the long decay phase seen also over Gale crater [6]. Figure 2 presents an evolution of spatial daytime dust distribution from Ls = 160° to 280° in MY 34. Similar to MY25, some signs of the onset of MY34 storm are observed by PFS just after the northern autumn equinox at Ls ~ 190° (Fig.1, 2c). Trace Gas Orbiter (TGO) finds the onset of this GDS Ls ~ 188° [7]. We start observing dust increases up to around 0.4 over Aonia Terra (50°S; 280°E), northern rim of Hellas and Noachis Terra (50°S; 10°E) (Fig.2a). Relatively large dust loads are also observed by ACS-TGO below 15 km at Ls = 168.75° in the latitude range: 39°S - 43°S [7], particularly around Hellas. Dust activity is then observed westward of Argyre (Aonia Terra) with opacity around 0.6 (Fig. 2b). Dust is also distributed over a wider region extended from 280°E to 200°E at around 50°S (Sirenum Terra). Acidalia (30°N–60°N, 300°E–360°E) and Utopia (30°N–60°N, 80°E–140°E) Planitia are regions where some precursor dust storms were imaged at Ls = 181° by MARCI [8]. From Ls = 160° to 180° (Fig.2a,b) dust activity is indeed observed by PFS where precursor dust storms were found by MARCI. Regions poleward of Utopia and Acidalia Planitia are covered by dust with opacities larger than 0.3 – 0.4. Thus, we possibly observe four regions where precursor dust storms could originate before Ls = 181° including Acidalia and Utopia Planitia imaged by MARCI, Hellas basin and Aonia – Sirenum Terra. In spite of sparse data in next Ls interval (Fig.2c), we are able to note the dust increases in Chryse Planitia (330°E; 10°N) and Arabia Terra (20°E; 20°N).

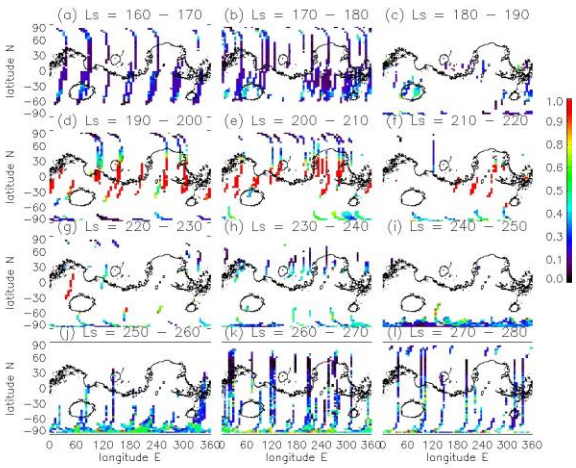

Figure 2: Spatial distribution of dayside (8-19LT) dust opacity normalized at 6.1 mbar of MY 34.

These regions are located near the meridional corridors for the dust transport from the north to the south [9]. We also observe larger opacity in the eastern half of the Hellas basin compared to the western counterpart. MARCI [10,11] showed substantial dust lifting originating along the edges of the receding southern polar cap by Ls ~ 188°. By Ls ~ 193° dust becomes distributed globally [11, 6]. PFS also observes a rapid increase of dust opacity (up to 4 or more) from Ls = 190° - 210° between 45°S to 45°N (Fig. 2d,e). The decay phase starts at Ls ~ 205° [12]. Despite the poor spatial coverage, PFS observes significant opacities (around 1.5) at some locations from Ls = 210° - 230° (Fig. 2f,g). Then the atmospheric dust progressively decreases by settling down on the surface (Fig. 2h). It is worth to note that dust activity occurs also close to the southern polar regions starting from Ls = 200° and continues until Ls = 280° (Fig. 2i,j,k,l).

3. Summary and Conclusions

In this study we collected dust opacities obtained from measurements performed by TES and PFS during 3 GDSs. We describe some detail of the spatial and seasonal evolution of dust content in the atmosphere during the MY 34 storm.

References

[1] Strausberg M.J., et al.: Observations of initiation and evolution of the 2001 Mars global dust storm, J. Geophys. Res., 110 (E02006), 10.1029/2004JE002361, 2005.

[2] Smith M. D., et al.: Thermal Emission Spectrometer Observations of Martian Planet-Encircling Dust Storm 2001A, Icarus, 157, 259 – 263, 2002.

[3] Cantor B. A.: MOC observations of the 2001 Mars planet-encircling dust storm, Icarus, 186, 60 – 96, 2007.

[4] Wolkenberg P., et al.: Characterization of dust activity on Mars from MY27 to MY32 by PFS-MEX observations, Icarus, 310, 32 – 47, 2018

[5] Smith M. D.: THEMIS observations of Mars aerosol optical depth from 2002 – 2008, Icarus, 202, 444 – 452, 2009.

[6] Guzewich, S. D., et al.: Mars Science Laboratory observations of the 2018/Mars year 34 global dust storm. Geophysical Research Letters, 46, 2019

[7] Vandaele et al.: Martian dust storm impact on atmospheric H2O and D/H observed by ExoMars Trace Gas Orbiter, Nature, 568, 521–525, 2019

[8] Malin, M. C., et al.: MRO MARCI weather report for the week of 21 May 2018–27 May 2018, Malin Space Science Systems Captioned Image Release, MSSS-532, 2018a. http://www.msss.com/msss_images/2018/05/30/

[9] Wang H. and M. I. Richardson: The origin, evolution, and trajectory of large dust storms on Mars during years 24-30 (1999 – 2011), *Icarus*, 251, 112 – 127, 2015.

[10] Malin, M. C., et al.: MRO MARCI weather report for the week of 4 June 2018–10 June 2018, Malin Space Science Systems Captioned Image Release, MSSS-534, 2018b. http://www.msss.com/msss_images/2018/06/13/

[11] Malin, M. C., et al.: MRO MARCI weather report for the week of 11 June 2018–17 June 2018, Malin Space Science Systems Captioned Image Release, MSSS-535, 2018c. http://www.msss.com/msss_images/2018/06/20/

[12] Malin, M. C., et al.: MRO MARCI weather report for the week of 2 July 2018–8 July 2018, Malin Space Science Systems Captioned Image Release, MSSS-538, 2018d. http://www.msss.com/msss_images/2018/07/11/